

LETTER TO THE EDITOR

Spin fluctuation-induced superconductivity in κ -BEDT-TTF compounds

Hisashi Kondo and Tôru Moriya

Department of Physics, Faculty of Science and Technology, Science University of Tokyo, Noda 278-8510, Japan

Received 8 June 1999

Abstract. Spin fluctuation-induced superconductivity in quasi-two dimensional organic compounds, κ -BEDT-TTF salts, is investigated within a fluctuation exchange (FLEX) approximation using a half-filled Hubbard model with a right-angled isosceles triangular lattice (transfer matrices $-\tau, -\tau'$), extending a previous work above T_c . An energy gap of A_2 or $(x^2 - y^2)$ -type develops with decreasing temperature below T_c more rapidly than in the BCS model. The calculated dynamical susceptibilities enough below T_c show sharp resonance peaks like those in certain cuprates superconductors. The calculated nuclear spin-lattice relaxation rate $1/T_1$ shows a T^3 behaviour below T_c in accordance with experiment. Estimated values of $1/T_1$ are roughly consistent with experimental results. A prediction is made for the doping concentration dependence of T_c and the antiferromagnetic and superconductive instability points are calculated in the U/τ against τ'/τ plane.

Recent theoretical investigations indicate that the superconductivity in quasi-two dimensional organic compounds κ -(BEDT-TTF) $_2X$ (where $X = \text{Cu}\{\text{N}(\text{CN})_2\}X'$, $X' = \text{Cl}, \text{Br}$) can be explained in terms of the spin fluctuation mechanism [1–5]. The calculated values for the transition temperature T_c as well as the d-wave character of the order parameter seem to be consistent with the existing experimental results [6–11].

In a previous paper we have reported the results of calculations for T_c and the normal state properties of these compounds by using a Hubbard model consisting of dimer orbitals [1]. The purpose of the present communication is to report on the results of our extended calculations mainly to include the superconducting state.

The model and the approach are the same as those discussed in [1]. We use a half-filled Hubbard model with a right-angled isosceles triangular lattice consisting of the anti-bonding dimer orbitals with the inter-dimer transfer integrals $-\tau$ and $-\tau'$ as shown in figure 1. The estimated values for the transfer integrals are $\tau \sim 0.07$ eV and $\tau'/\tau \sim 0.8$ [12, 13]. We use the fluctuation exchange (FLEX) approximation where the dynamical susceptibilities are calculated within the renormalized random phase approximation (RRPA) and the normal and the anomalous self-energies are approximated by the simplest ones including a spin fluctuation propagator without vertex corrections. This approximation has been successful in many previous investigations on high- T_c cuprates, etc [14–21] and recent studies on the vertex corrections seem to indicate that its effects will not seriously modify the FLEX results [22].

Before reporting on the results below T_c we show in figure 2 the calculated phase boundaries, in the U/τ against τ'/τ plane, between the paramagnetic metallic (PM) and the antiferromagnetic (AF) phases and between PM and the superconductive (SC) phases. The former is obtained from the points where the value of $1/\chi_Q$ extrapolated to $T = 0$

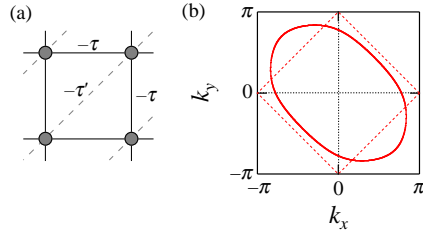


Figure 1. (a) The model unit cell and the transfer integrals. (b) Unperturbed Fermi surface for $\tau'/\tau = 0.8$. Dashed lines show the antiferromagnetic zone boundary.

vanishes. The latter is obtained from the points of vanishing T_c calculated by extrapolating the T_c/τ vs. U/τ plots, shown in the inset of figure 2, using the Padé approximants [23]. This result, being consistent with the conjectures in [1], shows that the AF and SC instabilities compete with each other and the latter wins for the values of τ'/τ larger than ~ 0.3 . In other words, the d-wave superconductivity appears near the antiferromagnetic instability only when the electronic structure is favourable; an antiferromagnetic instability is not necessarily accompanied by a d-wave superconductivity. With increasing U/τ from a superconducting instability point we expect a phase transition to an antiferromagnetic state. The phase boundary between the superconducting and antiferromagnetic phases must be obtained by comparing the free energies of the two phases, since the phase transition is naturally of the first order. This task is left for future studies.

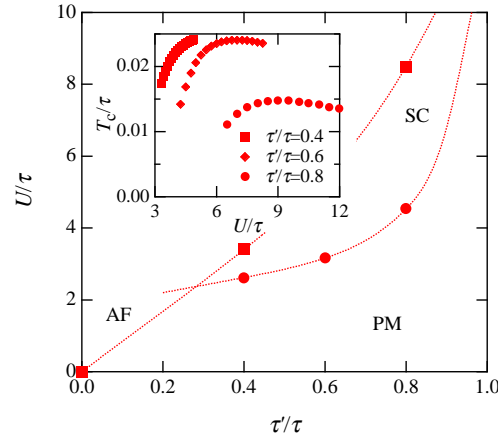


Figure 2. Instability points of the paramagnetic state against superconductivity and antiferromagnetism. Inset shows the results of an improved calculation for T_c/τ vs. U/τ .

Figure 3 shows the calculated values of T_c for $\tau'/\tau = 0.8$ for various values of n , the number of electrons per site, and U/τ . These results may be regarded as a prediction for the doping concentration-dependence of T_c in κ -(BEDT-TTF) $_2X$.

Now we discuss the properties in the superconducting state. We first show in figures 4(a) and 4(b) the anisotropy and the temperature dependences of the gap function $\Delta_k =$

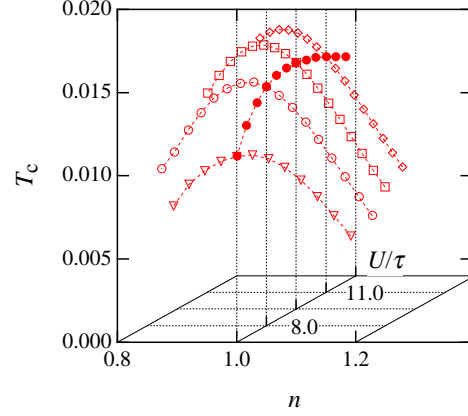


Figure 3. Electron number (doping concentration) dependence of T_c/τ for $\tau'/\tau = 0.8$.

$\text{Re}\{\Delta(\mathbf{k}, \Delta_{\mathbf{k}})\}$, respectively, where the gap function is defined by

$$\Delta(\mathbf{k}, \omega) = \frac{\Sigma^{(2)}(\mathbf{k}, \omega + i\eta)}{Z(\mathbf{k}, \omega)}$$

$$\omega Z(\mathbf{k}, \omega) = \omega - \frac{1}{2} [\Sigma^{(1)}(\mathbf{k}, \omega + i\eta) - \Sigma^{(1)}(\mathbf{k}, -\omega - i\eta)] \quad (1)$$

$\Sigma^{(1)}$ and $\Sigma^{(2)}$ being the normal and the anomalous self-energies, respectively. The symmetry of the gap function is clearly of A_2 or $(x^2 - y^2)$ -type and its amplitude develops more rapidly than in the standard BCS model below T_c . Figure 5 shows the renormalized density of states at various temperatures, indicating how it is influenced by the d-wave gap formation with lowering temperature. As is expected from figure 4 the energy gap in the density of states develops rapidly with decreasing temperature, approaching close enough to a limiting result at around $T_c/2$.

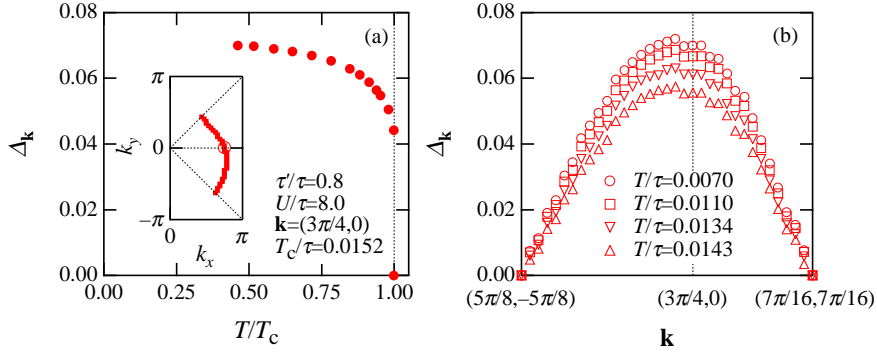


Figure 4. Calculated gap function. (a) Temperature dependence of $\Delta_{\mathbf{k}}$, with \mathbf{k} indicated by an open circle on the Fermi line shown in the inset. (b) Anisotropy or the wave vector-dependence of $\Delta_{\mathbf{k}}$, with \mathbf{k} on the Fermi line shown in the inset of (a).

The calculated dynamical susceptibilities well below T_c show strong resonance peaks around (π, π) and $(\pi, -\pi)$, just as in the calculations for the high- T_c cuprates. Similarly to

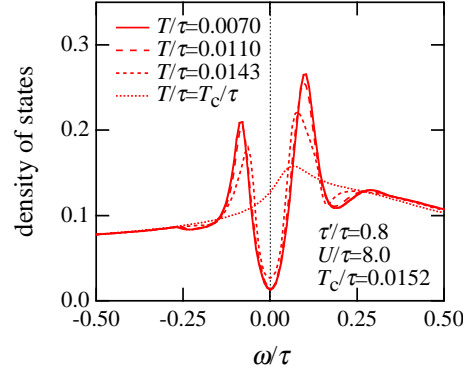


Figure 5. Density of states at various temperatures.

those in cuprates we interpret this resonance peak as a spin exciton [15, 20], a bound pair of an electron and a hole excited across the energy gap. Figure 6 shows the imaginary part of the dynamical spin susceptibility at $\mathbf{q} = (\pi, \pi)$ at various temperatures. We see how the resonance peak develops from a broad spectrum in the normal state. Figure 7 shows the dispersion and broadening of the spin excitons. The resonance peak position ω_q and the width γ_q are given by

$$1 - U \text{Re} \bar{\chi}_s(\mathbf{q}, \omega_q) = 0$$

$$\gamma_q = \frac{\text{Im} \bar{\chi}_s(\mathbf{q}, \omega_q)}{\left\{ \partial \text{Re} \bar{\chi}_s(\mathbf{q}, \omega) / \partial \omega \right\}_{\omega=\omega_q}} \quad (2)$$

with

$$\bar{\chi}_s(\mathbf{q}, i\omega_m) = -\frac{T}{N_0} \sum_{\mathbf{k}, n} [G(\mathbf{k} + \mathbf{q}, i\omega_n + i\omega_m) G(\mathbf{k}, i\omega_n) + F(\mathbf{k} + \mathbf{q}, i\omega_n + i\omega_m) F(\mathbf{k}, i\omega_n)] \quad (3)$$

where ω_m and ω_n are the Bose and Fermi Matsubara frequencies, respectively, and $G(\mathbf{k}, i\omega_n)$ and $F(\mathbf{k}, i\omega_n)$ are the renormalized normal and anomalous Green functions, respectively. The resonance peak appears only in limited regions of the \mathbf{q} -space around (π, π) and $(\pi, -\pi)$. We show in figure 8 the temperature variation of the \mathbf{q} -integrated intensity spectrum. It is desirable to have the corresponding neutron inelastic scattering experiments on single crystals in future although such an experiment, with a deuterized sample, does not seem to be very easy.

The nuclear spin-lattice relaxation rate can be calculated from the following general formula [24] using the FLEX dynamical susceptibilities:

$$\frac{1}{T_1} = \frac{\gamma_N^2 T}{N_0} \sum_{\mathbf{q}} |A_{\mathbf{q}}|^2 \frac{\text{Im} \chi^{-+}(\mathbf{q}, \omega_0)}{\omega_0} \quad (4)$$

where γ_N is the nuclear gyro-magnetic ratio, $A_{\mathbf{q}}$ the Fourier \mathbf{q} -component of the hyperfine coupling constant, and ω_0 the resonance frequency. We may neglect the \mathbf{q} -dependence of the hyperfine coupling constant which is anisotropic at the site of ^{13}C . According to [8] the principal values parallel and perpendicular to the direction of the $^{13}\text{C}=^{13}\text{C}$ bond are $a + 2B$ and $a - B$, respectively, with $a = 1.3 \text{ kOe } \mu_{\text{B}}^{-1}$ and $B = 2.1 \text{ kOe } \mu_{\text{B}}^{-1}$ for one spin per molecule; thus these values should be divided by 2 for one spin per dimer. For experimental results under the

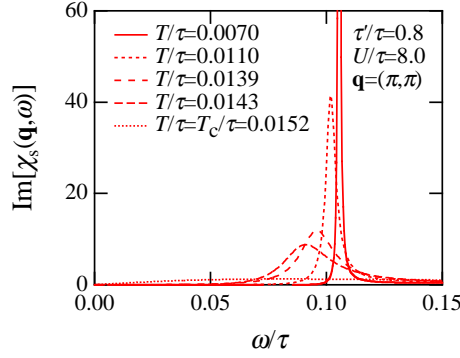


Figure 6. Calculated imaginary part of the dynamical susceptibility for $q = (\pi, \pi)$ at various temperatures.

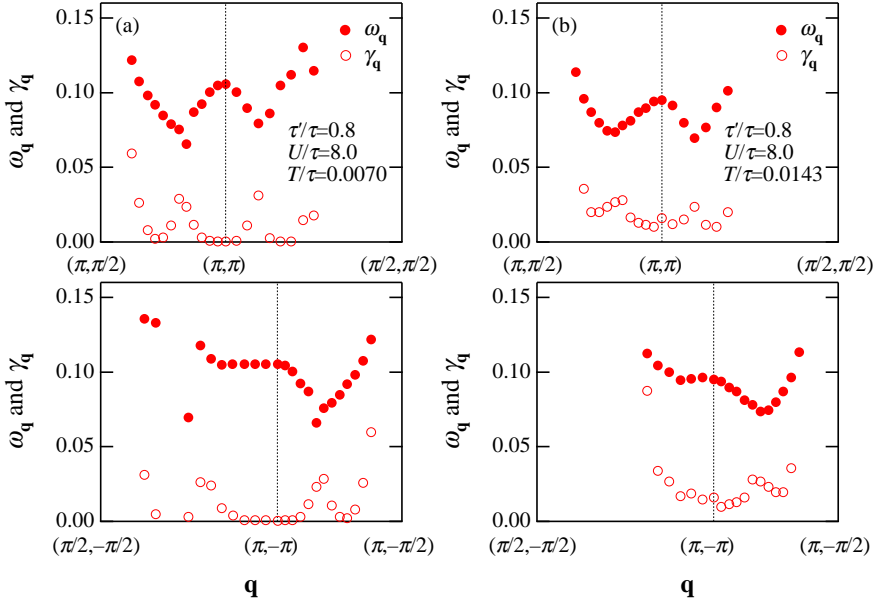


Figure 7. Dispersion and broadening of the resonance peak or the spin excitons. (a) $T/\tau = 0.0070$, (b) $T/\tau = 0.0143$.

magnetic field parallel to the conducting layer we may approximately replace $|A_q|^2$ in equation (4) with $[(a + 2B)^2 + (a - B)^2]/8$, since the C=C direction is nearly perpendicular to the layer. The result of calculation using this value for the coupling constant is shown in figure 9. The T^3 dependence of the relaxation rate below T_c as observed experimentally is well reproduced [7, 9, 10]. The order of magnitude also seems reasonable, in view of the approximate nature of the calculation. The observed values of $1/T_1 T$ above T_c has a peak at $T = T^* \sim 50$ K. Above this temperature T^* the system shows insulating behaviour while the system is metallic below T^* . Thus above T^* we had better use the Heisenberg model with the Anderson superexchange.

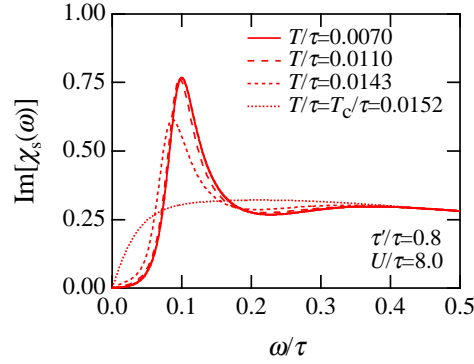


Figure 8. q -integrated spectrum of the imaginary part of the dynamical susceptibility.

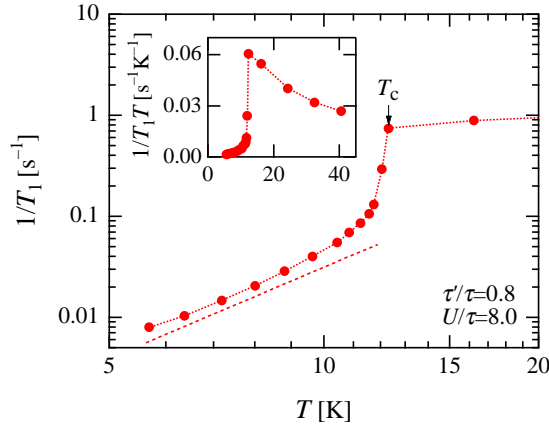


Figure 9. Calculated nuclear spin-lattice relaxation rate $1/T_1$ (logarithmic plots). The dashed line indicates a T^3 behaviour. Inset shows $1/T_1 T$ (normal plots).

For $T^* > T > T_c$ the observed values for $1/T_1 T$ decrease with decreasing temperature, reminiscent of the pseudo-spin gap behaviours in high- T_c cuprates. This behaviour is hard to understand within the present model and approximation. One possible explanation may be given by considering a coexistence of spin density wave (SDW) fluctuations and a charge density wave (CDW) or its slow fluctuations, although further studies are necessary before drawing any conclusion.

In summary, we have studied the spin fluctuation-induced superconducting state of quasi-two dimensional κ -(BEDT-TTF) $_2X$ compounds by using a half-filled triangular Hubbard model within the FLEX approximation, extending the previous study above T_c . The energy gap of $(x^2 - y^2)$ -type develops below T_c more rapidly than in the BCS model. Resonance peaks in the dynamical susceptibility are predicted in limited regions of the q -space around (π, π) and $(\pi, -\pi)$. The observed T^3 behaviour of the nuclear spin-lattice relaxation rate $1/T_1$ is well reproduced with a reasonable order of magnitude. We have also predicted the doping concentration dependence of T_c in these compounds. Calculations of the SC and AF instability points in the U/τ against τ'/τ plane show that the former is favourable only for τ'/τ

larger than ~ 0.3 , indicating that an antiferromagnetic instability does not always accompany the d-wave superconductivity.

Finally we would like to emphasize that the present mechanism seems to be the only available mechanism to describe the anisotropic superconductivity in quasi-two-dimensional κ -type BEDT-TTF compounds [25]. Theoretical results seem to be generally consistent with available experimental results except for the pseudo-spin gap behaviour of $1/T_1$ above T_c [26]. Further experimental and theoretical investigations are desired to confirm this mechanism.

We would like to thank Dr S Nakamura and Dr T Takimoto for helpful discussions.

References

- [1] Kondo H and Moriya T 1998 *J. Phys. Soc. Japan* **67** 3695
- [2] Kino H and Kontani H 1998 *J. Phys. Soc. Japan* **67** 3691
- [3] Schmalian J 1998 *Phys. Rev. Lett.* **81** 4232
- [4] Vojta M and Dagotto E 1999 *Phys. Rev. B* **59** 713
- [5] Kuroki K and Aoki H cond-mat/9812026
- [6] Mayaffre H, Wzietek P, Lenoir C, Jérôme D and Batail P 1994 *Europhys. Lett.* **28** 205
- [7] Mayaffre H, Wzietek P, Jérôme D, Lenoir C and Batail P 1995 *Phys. Rev. Lett.* **75** 4122
- [8] Kawamoto A, Miyagawa K, Nakazawa Y and Kanoda K 1995 *Phys. Rev. Lett.* **74** 3455
- [9] De Soto S M, Slichter C P, Kini A M, Wang H H, Geiser U and Williams J M 1995 *Phys. Rev. B* **52** 10364
- [10] Kanoda K, Miyagawa K, Kawamoto A and Nakazawa Y 1996 *Phys. Rev. B* **54** 76
- [11] Kanoda K 1997 *Physica C* **282-287** 299
- [12] Oshima K, Mori T, Inokuchi H, Urayama H, Yamochi H and Saito G 1988 *Phys. Rev. B* **38** 938
- [13] Kino H and Fukuyama H 1996 *J. Phys. Soc. Japan* **65** 2158
- [14] Bickers N E, Scalapino D J and White S R 1989 *Phys. Rev. Lett.* **62** 961
- [15] Pao C-H and Bickers N E 1994 *Phys. Rev. Lett.* **72** 1870
Pao C-H and Bickers N E 1995 *Phys. Rev. B* **51** 16310
- [16] Monthoux P and Scalapino D J 1994 *Phys. Rev. Lett.* **72** 1874
- [17] Dahm T and Tewordt L 1995 *Phys. Rev. B* **52** 1297.
- [18] Langer M, Schmalian J, Grabowski S and Bennemann K H 1995 *Phys. Rev. Lett.* **75** 4508
- [19] Koikegami S, Fujimoto S and Yamada K 1997 *J. Phys. Soc. Japan* **66** 1438
- [20] Takimoto T and Moriya T 1997 *J. Phys. Soc. Japan* **66** 2459
Takimoto T and Moriya T 1998 *J. Phys. Soc. Japan* **67** 3570
- [21] Kontani H and Ueda K 1998 *Phys. Rev. Lett.* **80** 5619
- [22] Monthoux P 1997 *Phys. Rev. B* **55** 15261
- [23] In solving the eigen value problem to obtain T_c , we took account of all the $(\mathbf{k}, i\omega_n)$ points by using the Lanczos algorithm, while 1000 important points were taken into account in the previous calculation in [1]. New values of T_c are somewhat larger than those in [1].
- [24] Moriya T 1963 *J. Phys. Soc. Japan* **18** 516
- [25] For example, any theories based on the t - J model can clearly be excluded since the half-filled electrons in these systems are in an intermediate coupling regime where an expansion in τ/U is inapplicable.
- [26] Recently the temperature dependences of the electrical resistivity and the Hall coefficient have reasonably been explained with essentially the same model as the present one and within the FLEX approximation by Kontani H, Kanki K and Ueda K *Phys. Rev. B* to be published; Kontani H and Kino H Private communication